Article

Static Output Feedback Control for Vehicle Platoons with Robustness to Mass Uncertainty

Fernando Viadero-Monasterio *[ID], Ramón Gutiérrez-Moizant [ID], Miguel Meléndez-Useros [ID] and María Jesús López Boada [ID]

Mechanical Engineering Department, Advanced Vehicle Dynamics and Mechatronic Systems (VEDYMEC), Universidad Carlos III de Madrid, Avenida de la Universidad, 30 (edificio Sabatini), Leganés, 28911 Madrid, Spain; ragutier@ing.uc3m.es (R.G.-M.); mmelende@ing.uc3m.es (M.M.-U.); mjboada@ing.uc3m.es (M.J.L.B.)
* Correspondence: fviadero@ing.uc3m.es

Abstract: Population growth and rising mobility demands have significantly increased traffic congestion and extended travel times. To address these challenges, traffic flow can be optimized by organizing vehicles into clusters, known as vehicle platoons, where cars travel closely together in a co-ordinated manner. Although the concept of vehicle platoon control holds great promise for improving traffic efficiency and reducing fuel consumption, its practical implementation faces several issues. Variations in vehicle specifications, such as differences in mass, can destabilize platoons and negatively impact overall performance. This paper introduces a novel method to maintain stable vehicle co-ordination despite such uncertainties. The proposed method utilizes a static output feedback control strategy, which simplifies the communication architecture within the platoon, as only partial state information from each vehicle is required. The simulation results demonstrate that this method effectively minimizes spacing errors and ensures platoon stability. This approach not only enhances safety but also improves traffic flow, making it a viable strategy for future intelligent transportation systems.

Keywords: vehicle platoon; intelligent transportation system; road safety; robust control; urban traffic

1. Introduction

The rapid growth of the global population and the expansion of urban areas have led to a significant increase in the demand for mobility over recent decades [1]. This has resulted in a range of critical issues, including worsening traffic congestion and increased pollution, which have a detrimental impact on the quality of life of individuals and communities [2]. The increase in the number of vehicles on the road has resulted in a greater prevalence of stop-and-go driving patterns, which have the effect of creating congestion, prolonging travel times, and increasing energy consumption [3]. Furthermore, these traffic congestion issues cause large groups of vehicles to remain stationary or move slowly in confined areas for extended periods, resulting in the concentrated emissions of harmful pollutants that have a significant impact on both human life and the natural environment [4].

In response to these challenges, vehicle platoon control has emerged as a promising solution to address issues of traffic congestion, inefficiency, and pollution [5–7]. The primary objective of a vehicle platoon is to organize traffic into co-ordinated groups of vehicles that travel closely together, maintaining safe distances while optimizing traffic flow [8]. A vehicle platoon consists of a lead vehicle, which may be autonomous or human-driven,

followed by multiple follower vehicles that are often fully autonomous or equipped to autonomously control only their longitudinal dynamics [9]. When the vehicle platoon is not fully autonomous, the longitudinal dynamics of each vehicle follower can be driverlessly controlled to adjust speed and spacing [10] while the driver remains responsible for certain tasks, such as steering.

One of the key challenges encountered in the design of vehicle platoon controllers is the issue of vehicle heterogeneity [11–15]. The mechanical characteristics of each vehicle in a platoon, including variations in mass, powertrain capabilities, and braking efficiency, result in differences in longitudinal dynamic behavior. These discrepancies present a challenge in synchronizing the motion of each vehicle effectively, as they can affect the desired consistency in spacing and the smooth acceleration and deceleration of the entire platoon [16]. Addressing this complexity is critical to ensure safe and co-ordinated platoon movement, particularly in scenarios characterized by a high degree of diversity in vehicle specifications.

Furthermore, the communication topology within a vehicle platoon is of significant importance in determining feasible control strategies and overall performance [17]. The communication framework defines the manner and the information each vehicle receives. The simplest communication topology, known as predecessor-following, provides each follower vehicle with only relative measurements, such as distance and velocity, about the vehicle directly in front [18]. While this approach is relatively easy to implement, it fails to ensure safe performance in practice [19]. Indeed, it compromises the string stability of the platoon by allowing tracking errors and disturbances to amplify as they propagate downstream, leading to increased oscillations and potential safety risks such as vehicle collisions across the platoon. In contrast, more advanced communication topologies, such as multiple-predecessor following or fully connected frameworks, can significantly enhance platoon performance by improving stability and responsiveness [20]. These topologies provide each vehicle with information from several or all preceding vehicles, enabling smoother and more co-ordinated maneuvers. However, this improved performance comes at a cost: these configurations are complex to implement and highly vulnerable to faults, such as network disruptions, cyber-attacks, or denial-of-service incidents, which can compromise the entire system's reliability and safety [21–23]. A commonly adopted robust solution for vehicle platoon control is the predecessor-leader following (PLF) topology [24]. In this configuration, each follower vehicle obtains real-time data about the leader's state through vehicle-to-vehicle (V2V) communication, while the state of its immediate predecessor is detected using onboard sensors, such as radar or lidar [25–27]. This hybrid approach enhances stability and safety by combining direct communication with reliable sensor-based feedback, enabling each vehicle to maintain precise spacing and respond effectively to changes in the platoon's movement.

The subject of vehicle platoon control is currently being investigated in depth by several researchers. In [28], a novel car-following model for adaptive cruise control vehicles using an enhanced intelligent driver model (IDM) is presented. However, the IDM is based on the PF topology, so it cannot guarantee that the platoon is string stable. In [29], a distributed model predictive control (MPC) algorithm was designed to control a platoon on curved roads. In [30], a cloud-edge co-operative scheme for heterogeneous vehicle platoon based on distributed MPC is proposed. In [31], an asynchronous stochastic self-triggered distributed MPC control scheme is proposed for vehicular platoon systems under coupled state constraints and additive stochastic disturbance. In [32], a distributed MPC for a heterogeneous vehicle platoon with an unknown input for leading vehicles is presented. In [33], Kalman filtering and MPC techniques are combined to control platoon formation. It is evident that there is a significant trend towards the control of vehicle

platoons through the implementation of MPC techniques. However, this approach may not be entirely feasible in practice due to the considerable computational costs associated with such techniques, which could potentially compromise the real-time implementation of the system [34]. Moreover, the deployment of MPC techniques demands a complete awareness of the state of the platoon at any given moment, in addition to inherently complex communication topologies [35]. Consequently, the utilization of MPC for platoon control is not recommended, and alternative output feedback control techniques should be employed. These techniques, such as PLF topology, possess the capability to adapt to reduced platoon knowledge [24].

Due to the aforementioned reasons, in this paper, we propose a novel vehicle platoon controller, which is designed to be robust against vehicle heterogeneity and external road disturbances. Since each vehicle only has access to limited platoon information, a static output feedback controller is designed to update the traction force on each vehicle. Closed-loop stability and robustness against external disturbances are guaranteed under Lyapunov and $\mathscr{H}_\infty$ criteria, respectively. Specifically, the contributions of this paper are summarized as follows:

- A methodology for the offline design of a controller under linear matrix inequality (LMI) conditions is proposed. This approach offers the advantage of eliminating the need for control gains to be recalculated during the execution time, which is in contrast to other methods, such as MPC [36]. The proposed controller is, therefore, capable of functioning in real time.
- $\mathscr{H}_\infty$ criteria are employed to design a vehicle platoon controller with guaranteed robustness against vehicle heterogeneity and external disturbances.
- By employing output feedback techniques within the predecessor-leader following (PLF) topology, the platoon controller guarantees the global stability of the entire system. This is accomplished even though the control signal for each vehicle is generated using only the relative information available to each follower vehicle, specifically from its immediate predecessor and the leader. This approach demonstrates the effectiveness of the controller in ensuring stability despite the constraints of the PLF topology.

The remainder of this paper is organized as follows. In Section 2, the mathematical model of the vehicle platoon is introduced. In Section 3, the methodology for designing the platoon controller is explained. Section 4 presents a series of tests that validate the effectiveness of the proposed controller. Section 5 concludes the paper.

Notation. The set of non-negative integers is denoted by $\mathbb{Z}_+$. The identity matrix is denoted as I. For a matrix X, $X^\top$ denotes its transpose. The function $\mathrm{He}(X)$ returns $\mathrm{He}(X) = X + X^\top$. If Y is a square matrix, $Y > 0$ denotes that Y is positive definite. In a symmetric matrix, the symbol $*$ indicates the transpose of the symmetric term. The function $\mathrm{diag}\left\{X_1, X_2\right\}$ retrieves a block-diagonal matrix composed of X_1 and X_2. If not stated, matrices are supposed to have compatible dimensions. For a variable, x, $\underline{x}$, and $\overline{x}$ denote the minimum and maximum values of x, respectively. Arguments are omitted when their meaning is clear.

2. Vehicle Platoon Model

The heterogeneous vehicle platoon presented in this paper is composed of $n + 1$ vehicles with different specifications, as depicted in Figure 1. The leader vehicle, designated as index 0, is externally human-controlled, while the following vehicles are indexed sequentially from 1 to n. Each vehicle in the platoon is assumed to be electric and powered by in-wheel motors (IWMs), providing rapid torque response; this enables the simplification of the model by neglecting the inertial lag effect in each following vehicle [37–39]. Aerodynamic drag, road slope, and rolling resistances act as external resistances. PLF

topology is selected for vehicle communication due to its strong potential for enhanced string stability [40]. In this configuration, each vehicle can measure relative states, such as distance and velocity, within the vehicle directly ahead while also receiving real-time state information from the lead vehicle via wireless communication.
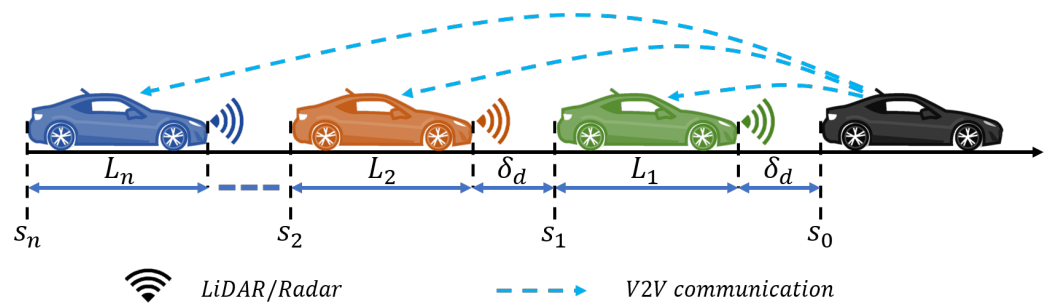

Figure 1. The PLF platoon considered for this work.

For each following vehicle in Figure 1, the longitudinal dynamics have to consider tire force, aerodynamic drag, rolling resistance, and grade resistance. The position and velocity of the *i*th vehicle are represented by s_i and v_i, respectively. Then, the longitudinal dynamic behavior of the *i*th vehicle is represented as in previous works, such as [38]:

$$\dot{s}_i = v_i$$
$$\dot{v}_i = \frac{1}{m_i}\left(F_{x,i} - F_{a,i} - F_{g,i} - F_{f,i}\right), \ i = 1, \ldots, n \tag{1}$$

The description of the model parameters and their typical ranges in automobiles are presented in Table 1. The resultant longitudinal tire force is denoted by F_x. The effect of external resistances is evaluated by F_a, F_g, and F_f, which are the aerodynamic, rolling, and grade resistances, respectively. These effects are calculated using

$$F_{a,i} = 0.5\rho C_{w,i}\Lambda_i(v_w - v_i)^2$$
$$F_{g,i} = m_i g \sin(\theta_i) \tag{2}$$
$$F_{f,i} = m_i g f_{r,i}\cos(\theta_i)$$

with $\rho = 1.293 \ \text{kg/m}^3$ and $g = 9.81 \ \text{m/s}^2$ denoting the air density and the acceleration of gravity, respectively.

Table 1. Minimum and maximum limits of vehicle parameters and external disturbances [41–43].

Symbol	Description	Unit	Min.	Max.
m_i	Vehicle mass	kg	800	2000
$C_{w,i}$	Coefficient of aerodynamic drag	−	0.29	0.39
Λ_i	Frontal cross-area	m²	1.58	2.9
$f_{r,i}$	Coefficient of rolling resistance	−	0.01	0.014
v_w	Wind speed	m/s	−12.9	12.9
θ_i	Road slope	°	−17.0 [a]	17.0 [a]
			−5.9 [b]	5.9 [b]

[a] Hilly road. [b] Highway and expressway.

The control input to give to each vehicle is the longitudinal tire force, F_x. In order to account for the possible mass variation from one vehicle to another, we define $F_{x,i}$ as

$$F_{x.i} = m^{\dagger} u_i \tag{3}$$

where $m^{\dagger}$ is the nominal vehicle mass

$$m^{\dagger} = \frac{\overline{m} + \underline{m}}{2} \tag{4}$$

Following (1)–(3), the longitudinal dynamics of the ith vehicle are expressed as

$$
\begin{aligned}
\dot{s}_i &= v_i \\
\dot{v}_i = a_i &= (\eta + \Delta_i \eta_m) u_i - 0.5 \frac{\eta + \Delta_i \eta_m}{m^{\dagger}} \rho C_{w,i} \Lambda_i (v_w - v_i)^2 \\
&\quad - g f_{r,i} \cos(\alpha_i) - g \sin(\alpha_i)
\end{aligned}
\tag{5}
$$

where Δ_i is the normalized nominal mass uncertainty that satisfies $|\Delta_i| \leq 1$, η is the nominal mass coefficient, and η_m is a coefficient that represents the maximum variation of the vehicle mass, which was obtained using

$$\eta = \frac{m^{\dagger}(\overline{m} + \underline{m})}{2\overline{m}\underline{m}}, \quad \eta_m = \frac{m^{\dagger}(\overline{m} - \underline{m})}{2\overline{m}\underline{m}} \tag{6}$$

In order to guarantee high traffic efficiency, a constant spacing policy is considered for this work. Following this consideration, the spacing and velocity errors between are expressed as

$$
\begin{aligned}
e_i &= s_{i-1} - s_i - L_i - \delta_d \\
\dot{e}_i &= v_{i-1} - v_i
\end{aligned}
\tag{7}
$$

where δ_d is the desired constant spacing between consecutive vehicles, which has been selected as $\delta_d = 15\ m$ for this work. It is evident that a collision between vehicles can be prevented as long as the inequality $e_i > -\delta_d$ is not violated.

In accordance with the PLF topology, a linear control method is selected for this work, which is in the form of

$$u_i = k_1(s_{i-1} - s_i - L_i - \delta_d) + k_2(v_{i-1} - v_i) + k_3(s_0 - s_i - \overline{L}_i - \overline{\delta}_{d,i}) + k_4(v_0 - v_i) \tag{8}$$

where k_j, $j = 1, \ldots, 4$ are control gains to be designed later. $\overline{L}_i$ represents the sum of every length of each vehicle located between the leader and the ith follower. $\overline{\delta}_{d,i}$ stands for the accumulated desired vehicle-free spacing between the leader and the ith follower, such that

$$\overline{L}_i = \sum_{j=1}^{i} L_j, \ \overline{\delta}_{d,i} = \sum_{j=1}^{i} \delta_d = i\delta_d \tag{9}$$

To achieve a compact representation of the heterogeneous platoon, a variable transformation is conducted by defining the tracking error with respect to the leader ξ_i as

$$\xi_i = s_0 - s_i - \overline{L}_i - \overline{\delta}_{d,i} \tag{10}$$

Now, under the definition of (10), the control input (8) is expressed as

$$u_i = k_1(\xi_i - \xi_{i-1}) + k_2(\dot{\xi}_i - \dot{\xi}_{i-1}) + k_3\xi_i + k_4\dot{\xi}_i \tag{11}$$

By putting together (5), (6), and (10), the following longitudinal dynamic model for the *i*th vehicle follower is obtained:

$$\dot{\xi}_i = v_0 - v_i$$

$$\ddot{\xi}_i = a_0 - (\eta + \Delta_i\eta_m)u_i + 0.5\frac{\eta + \Delta_i\eta_m}{m^{\dagger}}\rho C_{w,i}\Lambda_i(v_w - v_i)^2 \qquad (12)$$

$$+ gf_{r,i}\cos(\theta_i) + g\sin(\theta_i)$$

where a_0 serves to represent the acceleration of the leader vehicle. The system state and disturbance of the *i*th vehicle are denoted by ζ_i and ω_i, respectively, such that

$$\zeta_i = \begin{bmatrix} \xi_i \\ \dot{\xi}_i \end{bmatrix} \qquad (13)$$

$$\omega_i = a_0 + gf_{r,i}\cos(\theta_i) + 0.5\frac{\eta + \Delta_i\eta_m}{m^{\dagger}}\rho C_{w,i}\Lambda_i v_f^2 + g\sin(\theta_i)$$

By taking (13) into consideration, the model (12) is rewritten in the continuous-time state space, which is expressed as

$$\dot{\zeta}_i(t) = \mathcal{A}_i\zeta_i(t) + (\mathcal{B}_i + \mathcal{H}_i\Delta_iN_i)u_i(t) + \mathcal{B}_{\omega,i}\omega_i(t) \qquad (14)$$

with the continuous-time state-space matrices

$$\mathcal{A}_i = \begin{bmatrix} 0 & 1 \\ 0 & 0 \end{bmatrix}, \; \mathcal{B}_i = \begin{bmatrix} 0 \\ -\eta \end{bmatrix}, \; \mathcal{H}_i = \begin{bmatrix} 0 \\ 1 \end{bmatrix}, \; N_i = -\eta_m, \; \mathcal{B}_{\omega,i} = \begin{bmatrix} 0 \\ 1 \end{bmatrix}$$

Nevertheless, in order to facilitate the real-time application, it is preferred to transform model (14) into its discrete counterpart:

$$\zeta_i(k+1) = A_i\zeta_i(k) + (B_i + H_i\Delta_iN_i)u_i(k) + B_{\omega,i}\omega_i(k) \qquad (15)$$

where the new discrete-time state-space matrices are derived using the Euler discretization method, resulting in

$$A_i = I + \mathcal{A}_iT_d, \; B_i = \mathcal{B}_iT_d, \; H_i = \mathcal{H}_iT_d, \; B_{\omega,i} = \mathcal{B}_{\omega,i}T_d$$

Now, analyzing the behavior of the full platoon requires expanding system (15) so that each vehicle is included in a single model. A possible representation of full-platoon behavior in the discrete-time state space is

$$\zeta(k+1) = A\zeta(k) + (B + H\Delta N)u(k) + B_{\omega}\omega(k)$$
$$u(k) = KC_y\zeta(k) \qquad (16)$$
$$z(k) = C_z\zeta(k)$$

where z is a vector that represents the control objective, aiming to minimize each system state to effectively eliminate tracking errors. With the aim of minimizing the effect of external disturbances on every system state, the matrix C_z is selected as $C_z = I$. The state matrices are

$$A = \text{diag}(A_1, \ldots, A_n), \qquad B = \text{diag}(B_1, \ldots, B_n), \qquad H = \text{diag}(H_1, \ldots, H_n),$$

$$\Delta = \text{diag}(\Delta_1, \ldots, \Delta_n), \qquad N = \text{diag}(N_1, \ldots, N_n), \qquad B_{\omega} = \text{diag}(B_{\omega,1}, \ldots, B_{\omega,n})$$

$$\zeta = \begin{bmatrix} \zeta_1^{\top} & \zeta_2^{\top} & \cdots & \zeta_n^{\top} \end{bmatrix}^{\top}, \quad u = \begin{bmatrix} u_1 & u_2 & \cdots & u_n \end{bmatrix}^{\top}, \quad \omega = \begin{bmatrix} \omega_1 & \omega_2 & \cdots & \omega_n \end{bmatrix}^{\top}$$

and

$$K = I \otimes \begin{bmatrix} k_1 & k_2 & k_3 & k_4 \end{bmatrix}, \quad C_y = \begin{bmatrix} C_{11}^\top & C_{12}^\top & \dots & C_{n1}^\top & C_{n2}^\top \end{bmatrix}^\top,$$

$$C_{11} = \begin{bmatrix} I & 0 & \dots & 0 \end{bmatrix}, \qquad C_{12} = \begin{bmatrix} I & 0 & \dots & 0 \end{bmatrix},$$

$$C_{21} = \begin{bmatrix} -I & I & \dots & 0 \end{bmatrix}, \qquad C_{22} = \begin{bmatrix} 0 & I & \dots & 0 \end{bmatrix},$$

$$C_{n1} = \begin{bmatrix} 0 & \dots & -I & I \end{bmatrix}, \qquad C_{n2} = \begin{bmatrix} 0 & \dots & 0 & I \end{bmatrix},$$

3. Controller Design

This section presents a series of sufficient conditions for designing a vehicle platoon controller that is robust to the impacts of mass heterogeneity and external disturbances affecting the longitudinal dynamics of each vehicle.

First, define the change of variable

$$\begin{bmatrix} k_1 & k_2 & k_3 & k_4 \end{bmatrix} = \mathcal{F}\mathcal{G}^{-1} \tag{17}$$

where $\mathcal{F} \in \mathbb{R}^{1\times 4}$ and $\mathcal{G} \in \mathbb{R}^{4\times 4}$ are matrices to be designed later.

The application of the change in variable (17) on (16) returns the closed-loop vehicle platoon system model

$$
\begin{aligned}
\zeta(k+1) &= A\zeta(k) + (B + H\Delta N)u(k) + B_\omega \omega(k) \\
u(k) &= FG^{-1}C_y\zeta(k) \\
z(k) &= C_z\zeta(k)
\end{aligned}
\tag{18}
$$

where

$$F = I \otimes \mathcal{F}, \quad G^{-1} = I \otimes \mathcal{G}^{-1}$$

In order to obtain the matrices F and G, the following theorem provides sufficient conditions to design a robust SOF controller for the heterogeneous vehicle platoon (18).

Theorem 1. *The closed-loop vehicle platoon system* (18) *is asymptotically stable with an $\mathscr{H}_\infty$ performance index $\gamma > 0$ if there exists a matrix $Q > 0$, matrices F and G, and positive scalars $\mu > 0$ and $\varepsilon > 0$ such that the following LMI optimization problem returns feasible results:*

$$
\min \quad \gamma \quad \text{s.t.}
$$
$$
\begin{bmatrix}
-Q & \star & \star & \star & \star & \star & \star \\
0 & -\gamma^2 I & \star & \star & \star & \star & \star \\
AQ + BFC_y & B_\omega & -Q & \star & \star & \star & \star \\
C_yQ - GC_y & 0 & \varepsilon F^\top B^\top & -\varepsilon\mathrm{He}(G) & \star & \star & \star \\
C_zQ & 0 & 0 & 0 & -I & \star & \star \\
0 & 0 & -\mu H^\top & 0 & 0 & -\mu I & \star \\
NFC_y & 0 & 0 & \varepsilon NF & 0 & 0 & -\mu I
\end{bmatrix} < 0
\tag{19}
$$

Proof. Since $\Delta^\top \Delta \leq I$, when using the following matrix property [44]

$$\forall \mu > 0, \quad \mathscr{X}^\top \mathscr{Y} + \mathscr{Y}^\top \mathscr{X} \leq \mu \mathscr{X}^\top \mathscr{X} + \mu^{-1} \mathscr{Y}^\top \mathscr{Y} \tag{20}$$

the LMI (19) is equivalent to

$$
\begin{bmatrix}
-Q & \star & \star & \star & \star \\
0 & -\gamma^2 I & \star & \star & \star \\
AQ + (B + H\Delta N)FC_y & B_\omega & -Q & \star & \star \\
C_y Q - GC_y & 0 & \varepsilon F^\top (B + H\Delta N)^\top & -\varepsilon \mathrm{He}(G) & \star \\
C_z Q & 0 & 0 & 0 & -I
\end{bmatrix} < 0 \quad (21)
$$

The LMI (21) can be transformed following the Schur complement, which returns

$$
\begin{bmatrix}
-Q + QC_z^\top C_z Q & \star & \star & \star \\
0 & -\gamma^2 I & \star & \star \\
AQ + (B + H\Delta N)FC_y & B_\omega & -Q & \star \\
C_y Q - GC_y & 0 & \varepsilon F^\top (B + H\Delta N)^\top & -\varepsilon \mathrm{He}(G)
\end{bmatrix} < 0 \quad (22)
$$

Now, multiply the inequality (22) by

$$
\begin{bmatrix}
I & 0 & 0 & 0 \\
0 & I & 0 & 0 \\
0 & 0 & I & (B + H\Delta N)FG^{-1}
\end{bmatrix} \quad (23)
$$

on the left and by its transpose on the right in order to obtain

$$
\begin{bmatrix}
-Q + QC_z^\top C_z Q & \star & \star \\
0 & -\gamma^2 I & \star \\
AQ + (B + H\Delta N)FG^{-1}C_y Q & B_\omega & -Q
\end{bmatrix} < 0 \quad (24)
$$

Apply the change in variable $Q = P^{-1}$ and perform the congruent transform $\mathrm{diag}(P, I, I)$ to (24) such that

$$
\begin{bmatrix}
-P + C_z^\top C_z & \star & \star \\
0 & -\gamma^2 I & \star \\
A + (B + H\Delta N)FG^{-1}C_y & B_\omega & -P^{-1}
\end{bmatrix} < 0 \quad (25)
$$

By using the Schur complement once again, the LMI (25) is equivalent to

$$
\mathcal{W}^\top P \mathcal{W} + \begin{bmatrix}
-P + C_z^\top C_z & \star \\
0 & -\gamma^2 I
\end{bmatrix} < 0 \quad (26)
$$

where $\mathcal{W} = \begin{bmatrix} A + (B + H\Delta N)FG^{-1}C_y & B_\omega \end{bmatrix}$

By multiplying (26) by $\begin{bmatrix} \zeta^\top(k) & \omega^\top(k) \end{bmatrix}^\top$ on the left and its transpose on the right, the following expression is obtained:

$$
\Delta \mathcal{V}(k) + \mathcal{J}_{\mathcal{H}_\infty}(k) < 0 \quad (27)
$$

where $\Delta \mathcal{V}$ is the variation of the Lyapunov stability function candidate $\mathcal{V}(k) = \zeta^\top(k)P\zeta(k)$, and $\mathcal{J}_{\mathcal{H}_\infty}$ is the $\mathcal{H}_\infty$ robustness criterion, defined as [45]

$$
\begin{aligned}
& \Delta \mathcal{V}(k) < 0, \ \mathcal{J}_{\mathcal{H}_\infty}(k) < 0 \\
& \Delta \mathcal{V}(k) = \zeta^\top(k+1)P\zeta(k+1) - \zeta^\top(k)P\zeta(k) \\
& \mathcal{J}_{\mathcal{H}_\infty}(k) = z^\top(k)z(k) - \gamma^2 \omega^\top(k)\omega(k)
\end{aligned} \quad (28)
$$

From (28), it follows that the system (18) is stable under the Lyapunov criterion and is robust with the prescribed $\mathscr{H}_\infty$ performance γ; hence, the proof is complete. $\quad\square$

The subsequent theorem establishes a sufficient condition for the string stability of the platoon controller.

Theorem 2. *If the LMI (19) returns a feasible solution, the controller gains (17) guarantee that the platoon is string stable. Furthermore, if $\gamma < 1$, the platoon is strictly string stable.*

Proof. The proof can be found in [38] and is omitted here for simplicity. $\quad\square$

4. Results

In order to evaluate the performance of the proposed platoon controller, a simulation for a heterogeneous vehicle platoon composed of a leader and $n = 5$ vehicle followers was conducted. The longitudinal dynamics of each vehicle in the platoon were modeled according to (1) and (2). The simulations were performed using a computer equipped with an Intel Core i9-13900HX CPU and 32 GB of memory under the Matlab R2024a environment.

The mechanical specifications of each follower vehicle are presented in Table 2. The controller sampling time was chosen as $T_d = 0.01$ s. Following Theorem 1, a feasible controller was found with the $\mathscr{H}_\infty$ performance $\gamma = 0.5$. To this end, Matlab LMI solvers were employed. The control gains presented in (8) have been obtained as

$$k_1 = 1.17, \; k_2 = 1.12, \; k_3 = 9.71, \; k_4 = 10.48 \tag{29}$$

Table 2. Mechanical specifications of each follower vehicle in the platoon.

i	m_i	$C_{w,i}$	Λ_i	$f_{r,i}$
1	1400 kg	0.299	1.78 m^2	0.0106
2	1600 kg	0.3178	2.86 m^2	0.0117
3	1200 kg	0.3447	2.84 m^2	0.0137
4	1500 kg	0.3858	2.22 m^2	0.0132
5	1350 kg	0.3865	2.63 m^2	0.0138

Regarding the external disturbances that affect the longitudinal vehicle dynamics, the road slope and wind speed are defined as $\theta = 1.5°$ and $v_w = 1.5$ m/s, respectively. These values remain constant during the simulation.

The vehicle platoon is initiated under the assumption that it begins in a steady state, thereby ensuring that tracking errors are zero. This guarantees a synchronized start across all vehicles [38].

Two scenarios are subject to evaluation. The first scenario simulates highway traffic in order to approximate an everyday driving situation in the platoon. The second scenario is designed to verify the platoon stability when the leader vehicle suddenly conducts an emergency braking maneuver.

4.1. Scenario 1—Highway Driving

The objective of this scenario is to evaluate the stability of a vehicle platoon as the velocity of the leading vehicle varies during the course of a highway journey. The leader of the platoon follows the velocity and acceleration profiles presented in Figure 2.
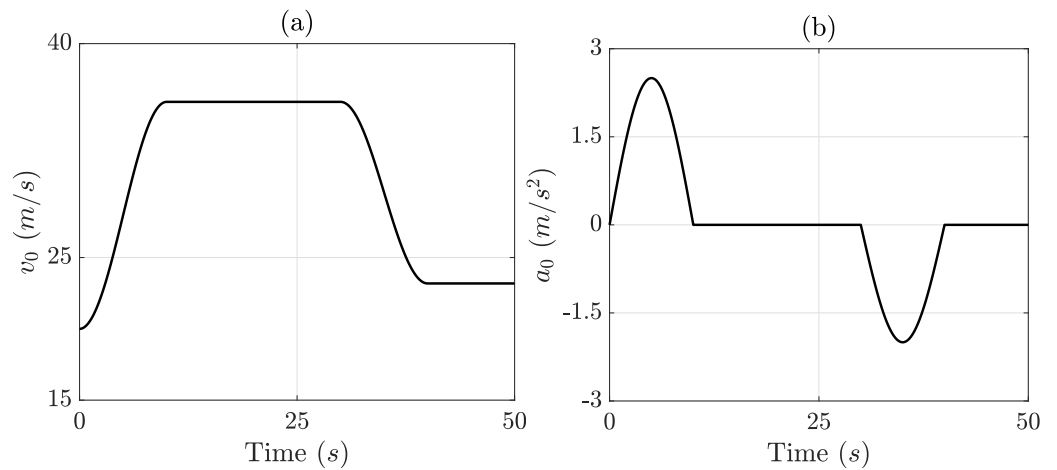
Figure 2. Leader profiles during scenario 1. (**a**) Velocity; (**b**) acceleration.

The position of the vehicles in the platoon under this scenario is presented in Figure 3. Since the simulated trajectories do not intersect each other, vehicle collisions do not happen, which ensures traffic safety. The platoon tracking errors over time are shown in Figure 4. It can be seen that separation errors tend to decrease when propagated downstream of the platoon, i.e., $|e_1| > |e_2| > \cdots > |e_n|$, which proves that the vehicle platoon has string-stable behavior. The rapid response capability of the platoon controller is demonstrated since the velocity tracking errors remain under 0.065 m/s during the course of the simulation.
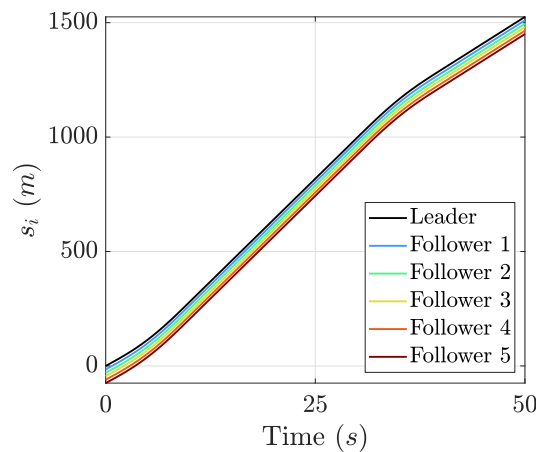
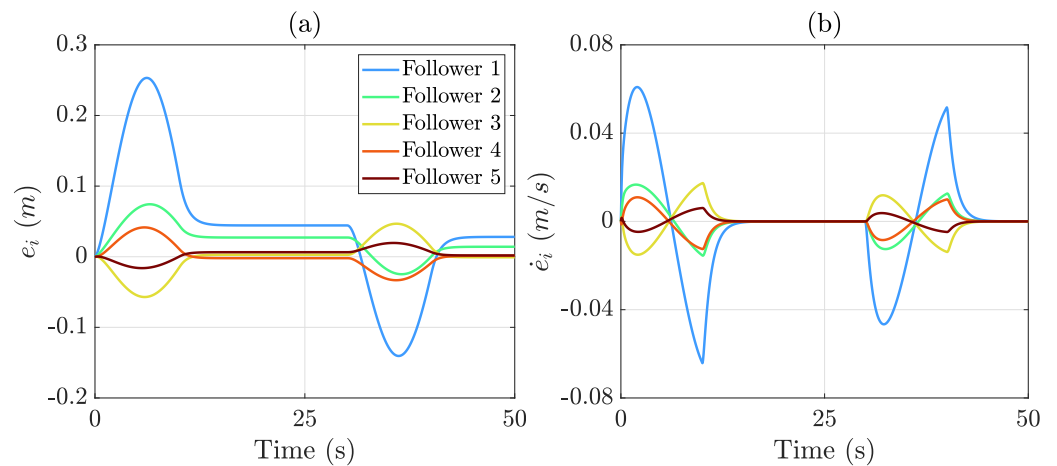**Figure 3.** Position of the vehicles in the platoon during scenario 1.

Figure 4. Tracking error evolution during scenario 1. (**a**) Separation error; (**b**) speed error.

In order to evaluate the performance of the platoon controller, the maximum and root mean square (RMS) values of the separation and velocity errors were evaluated. In the case of a set of n values $\{x_1, x_2, \ldots, x_n\}$, the RMS is calculated using

$$x_{RMS} = \sqrt{\frac{1}{n}\sum_{i=1}^{n} x_i^2} \tag{30}$$

Figure 5 presents the maximum and RMS values for the spacing error of each vehicle in the platoon. A maximum tracking error of 0.25 m is found for the first follower. The spacing error reduces when propagated downstream of the platoon, finding that the last follower reaches a maximum separation error below 0.02 m, which proves the effectiveness of the proposed method. Velocity tracking performance is introduced in Figure 6. The maximum velocity tracking error is 0.06 m/s for the first follower, while the last vehicle in the platoon has a maximum velocity tracking error below 0.01 m/s, which guarantees a smooth, stable movement in the vehicle string.
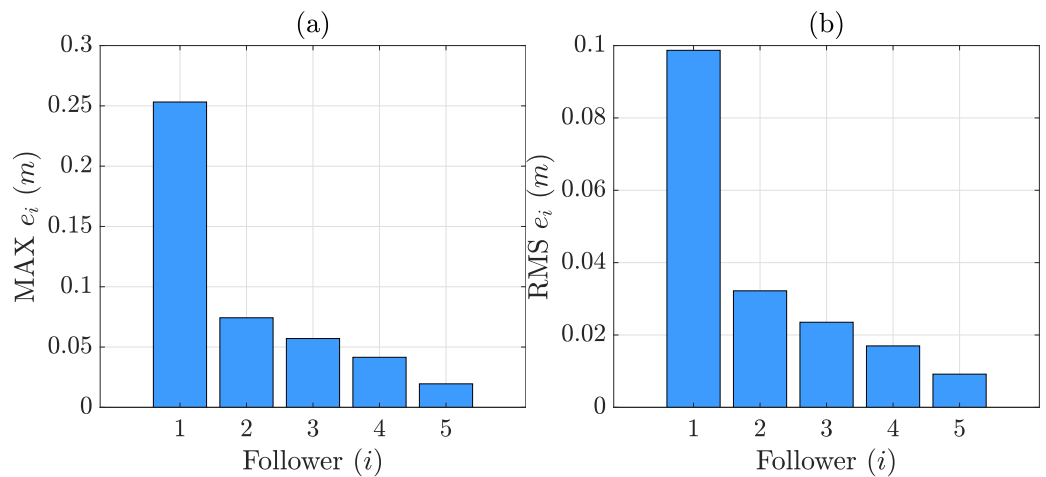

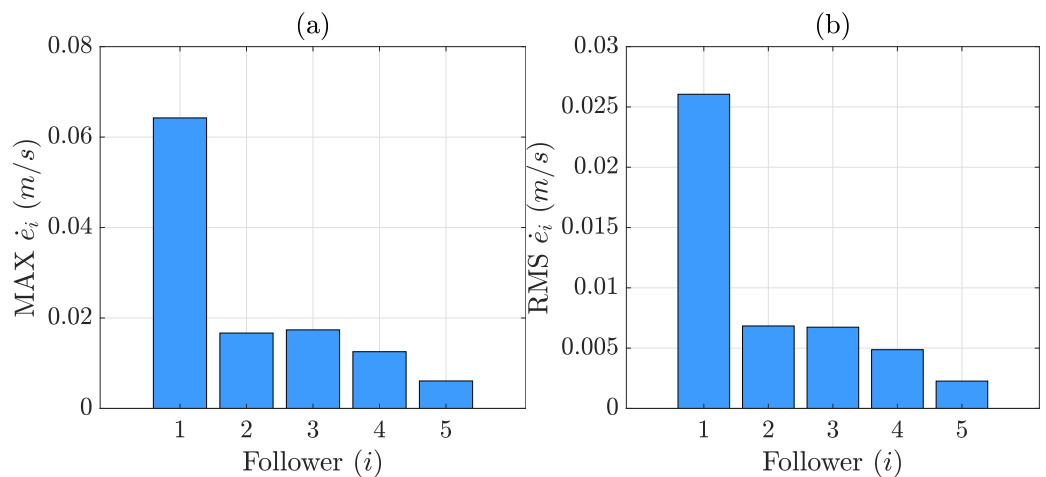**Figure 5.** Spacing errors during scenario 1. (**a**) MAX; (**b**) RMS.

Figure 6. Velocity errors during scenario 1. (**a**) MAX; (**b**) RMS.

4.2. Scenario 2—Emergency Braking

This scenario was designed to evaluate the ability of the platoon to co-operate and perform an emergency braking maneuver when required. The leader velocity and acceleration profiles are presented in Figure 7.
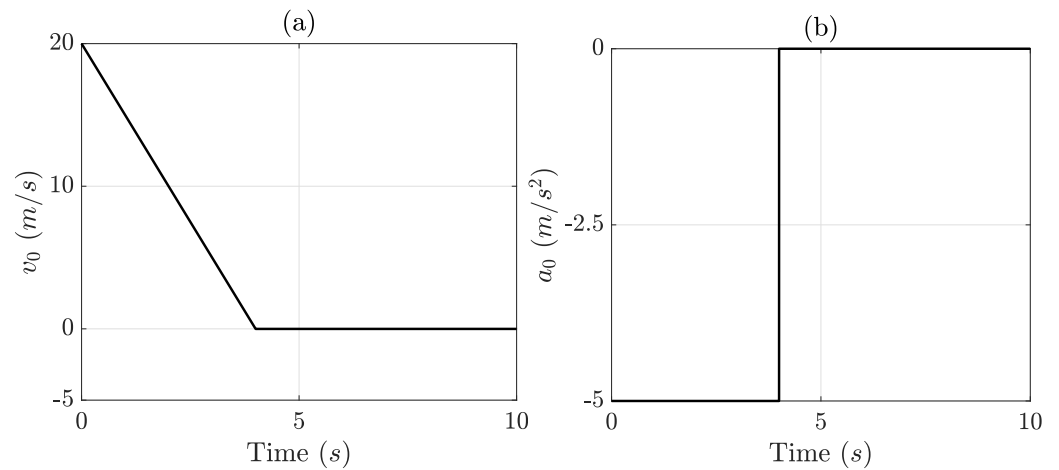
Figure 7. Leader profiles during scenario 2. (**a**) Velocity; (**b**) acceleration.

The longitudinal position of each vehicle in the platoon during the sudden braking maneuver is presented in Figure 8. It can be observed that vehicles maintain a constant separation between each other, thereby avoiding collisions. Spacing and velocity tracking errors are introduced in Figure 9. Once again, the string stability of the platoon is demonstrated, even in this challenging scenario. This is evidenced by a reduction in separation and velocity errors as they are propagated downstream within the platoon.
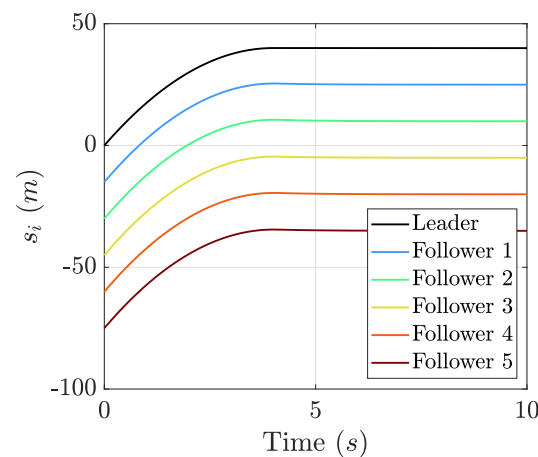

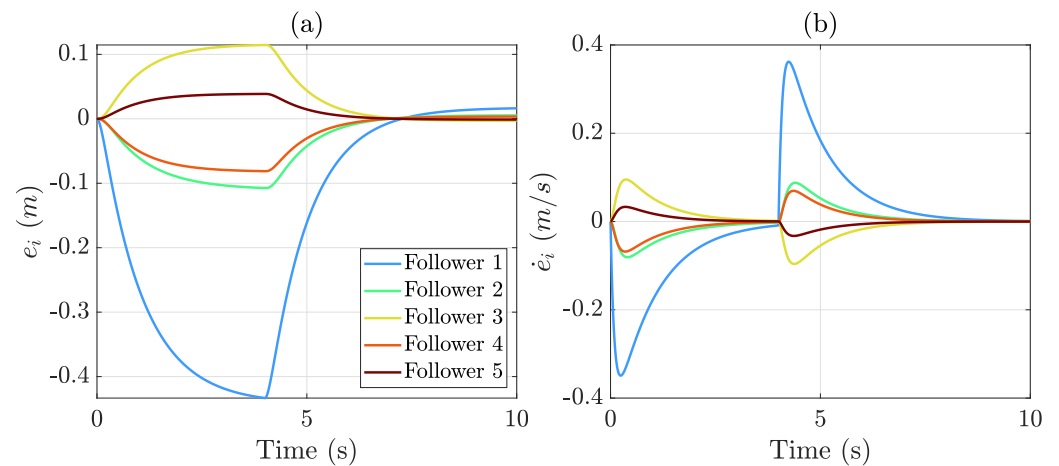**Figure 8.** Position of the vehicles in the platoon during scenario 2.

Figure 9. Tracking error evolution during scenario 2: (**a**) Separation error; (**b**) speed error.

The maximum and RMS values for the spacing error in this scenario are shown in Figure 10. The maximum tracking error remains below 0.45 m during all the tests, eliminating the possibility of collisions occuring. The velocity tracking performance is introduced in Figure 11. The maximum velocity tracking error remains below 0.4 m/s, which indicates the fast response of the vehicles in the platoon. The results demonstrate that the proposed method can ensure platoon stability and safety under an extreme maneuver.
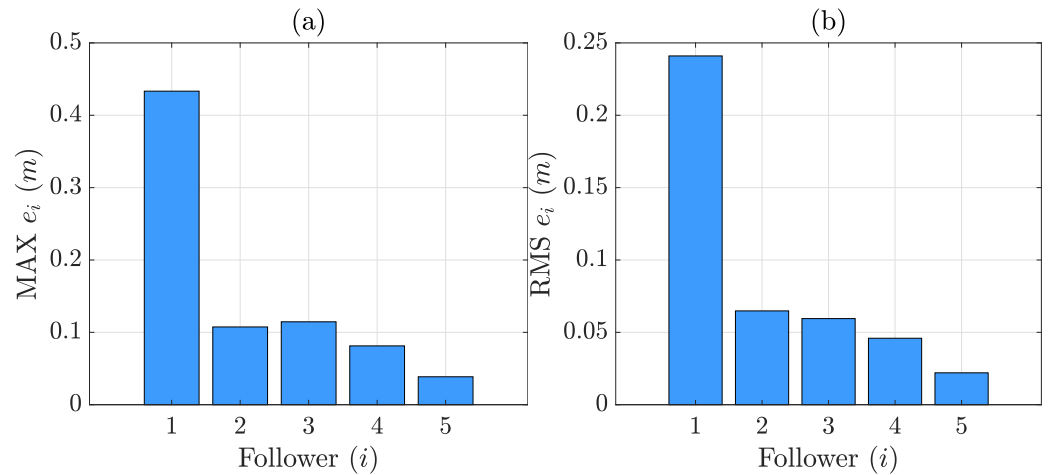
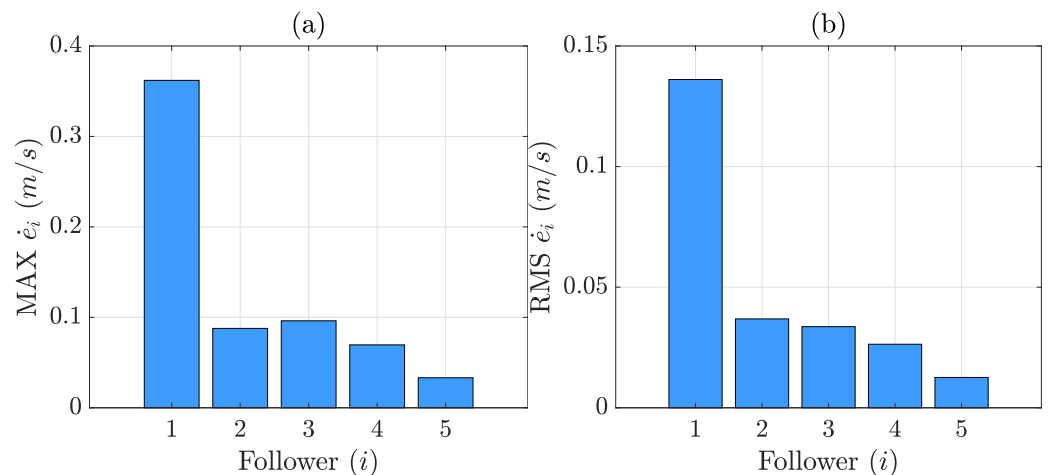**Figure 10.** Spacing errors during scenario 2. (**a**) MAX; (**b**) RMS.

Figure 11. Velocity errors during scenario 2. (**a**) MAX; (**b**) RMS.

5. Conclusions

This paper presents an investigation of the problem of robust vehicle platoon control, with a particular focus on the impact of mass variance on the overall heterogeneity of the system.

The platoon controller has been designed in the discrete-time domain, as this approach offers a more practical solution. The system is guaranteed to be stable in accordance with the Lyapunov criteria. The robustness of the proposed strategy towards external disturbances and measurement noise was investigated using the analysis of the $\mathcal{H}_\infty$ norm.

The proposed platoon controller was evaluated under two distinct conditions. The initial scenario involves an everyday driving situation in which the vehicle in the lead accelerates, and the subsequent vehicles must be able to maintain the same speed and reach a stationary position. Secondly, an emergency braking maneuver was conducted to test the safety and stability of the platoon under extreme conditions. The results demonstrate that the proposed method is highly reliable and capable of achieving maximum separation errors below 0.5 m. This ensures the avoidance of collisions between vehicles.

Future works will focus on the formulation of a strategic plan for the movement of the leader that takes road conditions into account with the objective of reducing the collective energy consumption of the platoon. In addition, a mechanism will be developed to ensure the integrity of the system. This mechanism will include a process for detecting false data injection and adapting to switching communication topologies [46].

Author Contributions: Conceptualization, F.V.-M., R.G.-M., M.M.-U. and M.J.L.B.; methodology, F.V.-M., R.G.-M., M.M.-U. and M.J.L.B.; software, F.V.-M., R.G.-M., M.M.-U. and M.J.L.B.; validation, F.V.-M., R.G.-M., M.M.-U. and M.J.L.B.; formal analysis, F.V.-M., R.G.-M., M.M.-U. and M.J.L.B.; investigation, F.V.-M., R.G.-M., M.M.-U. and M.J.L.B.; resources, F.V.-M., R.G.-M., M.M.-U. and M.J.L.B.; data curation, F.V.-M., R.G.-M., M.M.-U. and M.J.L.B.; writing—original draft preparation, F.V.-M., R.G.-M., M.M.-U. and M.J.L.B.; writing—review and editing, F.V.-M., R.G.-M., M.M.-U. and M.J.L.B.; visualization, F.V.-M., R.G.-M., M.M.-U. and M.J.L.B.; supervision, F.V.-M., R.G.-M., M.M.-U. and M.J.L.B.; project administration, F.V.-M., R.G.-M., M.M.-U. and M.J.L.B.; funding acquisition, F.V.-M., R.G.-M., M.M.-U. and M.J.L.B. All authors have read and agreed to the published version of the manuscript.

Data Availability Statement: The original contributions presented in the study are included in the article; further inquiries can be directed to the corresponding author.

Conflicts of Interest: The authors declare no conflicts of interest.

Abbreviations

The following abbreviations are used in this manuscript:

IWM	In-wheel motors
LMI	Linear matrix inequality
MPC	Model predictive control
PF	Predecessor following
PLF	Predecessor-leader following
RMS	Root mean square
V2V	Vehicle-to-vehicle

References

1. Alhameed, M.; Mahgoub, I.; Limouchi, E. Intelligent High-Awareness and Channel-Efficient Adaptive Beaconing Based on Density and Distribution for Vehicular Networks. *Electronics* **2024**, *13*, 891. [CrossRef]
2. Granà, A.; Curto, S.; Petralia, A.; Giuffrè, T. Connected Automated and Human-Driven Vehicle Mixed Traffic in Urban Freeway Interchanges: Safety Analysis and Design Assumptions. *Vehicles* **2024**, *6*, 693–710. [CrossRef]
3. Desai, J.; Saldivar-Carranza, E.D.; Sakhare, R.S.; Mathew, J.K.; Bullock, D.M. Impact of In-Cab Alerts on Connected Truck Speed Reductions in Indiana. *Vehicles* **2024**, *6*, 1857–1871. [CrossRef]
4. Kumar, K.N.; Roy, D.; Suman, T.A.; Vishnu, C.; Mohan, C.K. TSANet: Forecasting traffic congestion patterns from aerial videos using graphs and transformers. *Pattern Recognit.* **2024**, *155*, 110721. [CrossRef]
5. Liu, H.; Gong, L.; Chen, X.; Zheng, X.; Lv, C. Evaluating Efficiency of Connected and Autonomous Vehicles with Different Communication Topologies. *Electronics* **2023**, *12*, 3584. [CrossRef]
6. Jia, D.; Lu, K.; Wang, J.; Zhang, X.; Shen, X. A Survey on Platoon-Based Vehicular Cyber-Physical Systems. *IEEE Commun. Surv. Tutorials* **2016**, *18*, 263–284. [CrossRef]
7. Li, Q.; Chen, Z.; Li, X. A Review of Connected and Automated Vehicle Platoon Merging and Splitting Operations. *IEEE Trans. Intell. Transp. Syst.* **2022**, *23*, 22790–22806. [CrossRef]
8. Viadero-Monasterio, F.; Jiménez-Salas, M.; Meléndez-Useros, M.; López-Boada, M.J. Robust output feedback control for heterogeneous autonomous vehicle platoons. *DYNA-Ing. Ind.* **2024**, *99*, 487–492. [CrossRef]
9. Borneo, A.; Zerbato, L.; Miretti, F.; Tota, A.; Galvagno, E.; Misul, D.A. Platooning cooperative adaptive cruise control for dynamic performance and energy saving: A comparative study of linear quadratic and reinforcement learning-based controllers. *Appl. Sci.* **2023**, *13*, 10459. [CrossRef]

10. Rebelo, M.; Rafael, S.; Bandeira, J.M. Vehicle Platooning: A Detailed Literature Review on Environmental Impacts and Future Research Directions. *Future Transp.* **2024**, *4*, 591–607. [CrossRef]

11. Viadero-Monasterio, F.; Meléndez-Useros, M.; Jiménez-Salas, M.; Boada, B.L.; Boada, M.J.L. What are the most influential factors in a vehicle platoon? In Proceedings of the 2024 IEEE International Conference on Evolving and Adaptive Intelligent Systems (EAIS), Madrid, Spain, 23–24 May 2024; pp. 1–7. [CrossRef]

12. Li, M.; Li, S.; Luo, X.; Bai, Z. Nonsingular Terminal Sliding Mode Control for Vehicular Platoon Systems with Measurement Delays and Noise. *Computation* **2024**, *12*, 210. [CrossRef]

13. Kang, C.M. Disturbance Observer-Based Robust Cooperative Adaptive Cruise Control Approach under Heterogeneous Vehicle. *Energies* **2024**, *17*, 1429. [CrossRef]

14. Yin, J.; Hwang, S.H. Adaptive Speed Control Scheme Based on Congestion Level and Inter-Vehicle Distance. *Electronics* **2024**, *13*, 2678. [CrossRef]

15. Song, X.; Sun, Y.; Li, H.; Liu, B.; Cao, Y. Ecological cooperative adaptive control of connected automate vehicles in mixed and power-heterogeneous traffic flow. *Electronics* **2023**, *12*, 2158. [CrossRef]

16. Dong, H.; Wang, Y.; Li, X. Distributed Cooperative Synchronization and Tracking for Heterogeneous Platoons With Mixed-Order Nonlinear Vehicle Dynamics. *IEEE Access* **2024**, *12*, 110131–110145. [CrossRef]

17. Wang, X.; Xu, C.; Zhao, X.; Li, H.; Jiang, X. Stability and Safety Analysis of Connected and Automated Vehicle Platoon Considering Dynamic Communication Topology. *IEEE Trans. Intell. Transp. Syst.* **2024**, *25*, 13442–13452. [CrossRef]

18. Escobar, C.; Vargas, F.J.; Peters, A.A.; Carvajal, G. A Cooperative Control Algorithm for Line and Predecessor Following Platoons Subject to Unreliable Distance Measurements. *Mathematics* **2023**, *11*, 801. [CrossRef]

19. Bouadi, M.; Jiang, R.; Jia, B.; Zheng, S.T. String Stability Analysis of Cooperative Adaptive Cruise Control Vehicles Considering Multi-Anticipation and Communication Delay. *IEEE Trans. Intell. Transp. Syst.* **2024**, *25*, 11359–11369. [CrossRef]

20. Abolfazli, E.; Besselink, B.; Charalambous, T. Minimum Time Headway in Platooning Systems Under the MPF Topology for Different Wireless Communication Scenario. *IEEE Trans. Intell. Transp. Syst.* **2023**, *24*, 4377–4390. [CrossRef]

21. Sheik, A.T.; Maple, C.; Epiphaniou, G.; Dianati, M. A Comprehensive Survey of Threats in Platooning—A Cloud-Assisted Connected and Autonomous Vehicle Application. *Information* **2023**, *15*, 14. [CrossRef]

22. Durlik, I.; Miller, T.; Kostecka, E.; Zwierzewicz, Z.; Łobodzińska, A. Cybersecurity in Autonomous Vehicles—Are We Ready for the Challenge? *Electronics* **2024**, *13*, 2654. [CrossRef]

23. Han, Q.; Ma, J.; Zuo, Z.; Wang, X.; Yang, B.; Guan, X. Resilient Event-Triggered Control of Vehicle Platoon Under DoS Attacks and Parameter Uncertainty. *IEEE Trans. Intell. Veh.* **2024**, 1–9. [CrossRef]

24. Viadero-Monasterio, F.; Meléndez-Useros, M.; Jiménez-Salas, M.; Boada, B.L. Robust Adaptive Heterogeneous Vehicle Platoon Control Based on Disturbances Estimation and Compensation. *IEEE Access* **2024**, *12*, 96924–96935. [CrossRef]

25. Log, M.M.; Thoresen, T.; Eitrheim, M.H.; Levin, T.; Tørset, T. Using Low-Cost Radar Sensors and Action Cameras to Measure Inter-Vehicle Distances in Real-World Truck Platooning. *Appl. Syst. Innov.* **2023**, *6*, 55. [CrossRef]

26. Aung, N.H.H.; Sangwongngam, P.; Jintamethasawat, R.; Shah, S.; Wuttisittikulkij, L. A Review of LiDAR-based 3D Object Detection via Deep Learning Approaches towards Robust Connected and Autonomous Vehicles. *IEEE Trans. Intell. Veh.* **2024**, 1–23. [CrossRef]

27. Viadero-Monasterio, F.; Alonso-Rentería, L.; Pérez-Oria, J.; Viadero-Rueda, F. Radar-based pedestrian and vehicle detection and identification for driving assistance. *Vehicles* **2024**, *6*, 1185–1199. [CrossRef]

28. Bai, J.; Mao, S.; Lee, J.J. A novel car-following model for adaptive cruise control vehicles using enhanced intelligent driver model. *Transp. Lett.* **2024**, 1–17. [CrossRef]

29. Zuo, Z.; Yang, K.; Wang, H.; Wang, Y.; Wu, Y. Distributed MPC for Automated Vehicle Platoon: A Path-Coupled Extended Look-Ahead Approach. *IEEE Trans. Intell. Veh.* **2024**, 1–13. [CrossRef]

30. Zhao, J.; Ma, Y.; Dai, L.; Sun, Z.; Xia, Y. Cloud-Edge Cooperative Distributed MPC With Event-Triggered Switching Strategy for Heterogeneous Vehicle Platoon. *IEEE Trans. Veh. Technol.* **2024**, *73*, 14425–14437. [CrossRef]

31. Chen, J.; Wei, H.; Zhang, H.; Shi, Y. Asynchronous Self-Triggered Stochastic Distributed MPC for Cooperative Vehicle Platooning Over Vehicular Ad-Hoc Networks. *IEEE Trans. Veh. Technol.* **2023**, *72*, 14061–14073. [CrossRef]

32. Qiang, Z.; Dai, L.; Chen, B.; Li, K.; Xia, Y. Distributed model predictive control for heterogeneous vehicle platoon with unknown input of leading vehicle. *Transp. Res. Part C Emerg. Technol.* **2023**, *155*, 104312. [CrossRef]

33. Sun, N.; Liu, J.; Wang, P.; Xiao, G. Research on Intelligent Platoon Formation Control Based on Kalman Filtering and Model Predictive Control. *World Electr. Veh. J.* **2024**, *15*, 144. [CrossRef]

34. Viadero-Monasterio, F.; Nguyen, A.T.; Lauber, J.; Boada, M.J.L.; Boada, B.L. Event-Triggered Robust Path Tracking Control Considering Roll Stability Under Network-Induced Delays for Autonomous Vehicles. *IEEE Trans. Intell. Transp. Syst.* **2023**, *24*, 14743–14756. [CrossRef]

35. Feng, J.; Gao, Z.; Guo, B. State-Feedback and Nonsmooth Controller Design for Truck Platoon Subject to Uncertainties and Disturbances. *World Electr. Veh. J.* **2024**, *15*, 251. [CrossRef]

36. He, D.; Luo, J.; Du, H. Dynamic Negotiation-Based Distributed EMPC With Varying Consensus Speeds of Heterogeneous Electric Vehicle Platoons. *IEEE Trans. Control. Syst. Technol.* **2024**, *32*, 1495–1503. [CrossRef]

37. Adnane, M.; Nguyen, C.T.P.; Khoumsi, A.; Trovão, J.P.F. Real-Time Torque-Distribution for Dual-Motor Off-Road Vehicle Using Machine Learning Approach. *IEEE Trans. Veh. Technol.* **2024**, *73*, 4567–4577. [CrossRef]

38. Xu, L.; Zhuang, W.; Yin, G.; Bian, C. Stable Longitudinal Control of Heterogeneous Vehicular Platoon with Disturbances and Information Delays. *IEEE Access* **2018**, *6*, 69794–69806. [CrossRef]

39. Govers, W.; Yurtman, A.; Aslandere, T.; Eikelenberg, N.; Meert, W.; Davis, J. Time-Shifted Transformers for Driver Identification Using Vehicle Data. *IEEE Trans. Intell. Transp. Syst.* **2024**, *25*, 3767–3776. [CrossRef]

40. Luo, T.; Liu, X. Ecological cooperative merging control of heterogeneous electric vehicle platoons. *PLoS ONE* **2024**, *19*, e0309930. [CrossRef] [PubMed]

41. Rajamani, R. *Vehicle Dynamics and Control*; Springer Science & Business Media: Berlin/Heidelberg, Germany, 2011.

42. Lechner, G.; Naunheimer, H. *Automotive Transmissions: Fundamentals, Selection, Design and Application*; Springer Science & Business Media: Berlin/Heidelberg, Germany, 1999.

43. Gao, F.; Li, S.E.; Zheng, Y.; Kum, D. Robust control of heterogeneous vehicular platoon with uncertain dynamics and communication delay. *IET Intell. Transp. Syst.* **2016**, *10*, 503–513. [CrossRef]

44. Nguyen, A.T.; Rath, J.; Guerra, T.M.; Palhares, R.; Zhang, H. Robust Set-Invariance Based Fuzzy Output Tracking Control for Vehicle Autonomous Driving Under Uncertain Lateral Forces and Steering Constraints. *IEEE Trans. Intell. Transp. Syst.* **2021**, *22*, 5849–5860. [CrossRef]

45. Viadero-Monasterio, F.; Meléndez-Useros, M.; Jiménez-Salas, M.; Boada, B.L. Robust Static Output Feedback Control of a Semi-Active Vehicle Suspension Based on Magnetorheological Dampers. *Appl. Sci.* **2024**, *14*, 10336. [CrossRef]

46. Xiao, S.; Ge, X.; Han, Q.L.; Zhang, Y. Secure and collision-free multi-platoon control of automated vehicles under data falsification attacks. *Automatica* **2022**, *145*, 110531. [CrossRef]